Agricultural and Forest Meteorology 353 (2024) 110051

Contents lists available at ScienceDirect

Agricultural and Forest Meteorology

journal homepage: www.elsevier.com/locate/agrformet

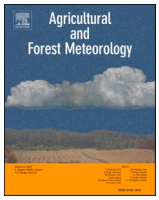

Varied responses of Amazon forests to the 2005, 2010, and 2015/2016 droughts inferred from multi-source satellite data

Xiaojun She [a,b], Yao Li [a,c,*], Wenzhe Jiao [d], Yuanheng Sun [b,e], Xiangnan Ni [b,f], Zhenpeng Zuo [b], Yuri Knyazikhin [b], Ranga B. Myneni [b]

[a] Chongqing Jinfo Mountain Karst Ecosystem National Observation and Research Station, School of Geographical Sciences, Southwest University, Chongqing 400715, China
[b] Department of Earth and Environment, Boston University, Boston, MA 02215, USA
[c] Zachry Department of Civil and Environmental Engineering, Texas A&M University, College Station, TX 77843, USA
[d] Department of Ecology and Conservation Biology, Texas A&M University, College Station, TX 77843, USA
[e] Environmental Information Institute, Navigation College, Dalian Maritime University, Dalian 116026, China
[f] Department of Earth and Environmental Sciences, Xi'an Jiaotong University, Xi'an, Shaanxi 710049, China

ARTICLE INFO

Keywords:
Drought
Amazon forests
Leaf area
Solar-induced chlorophyll fluorescence
Vegetation optical depth
Solar radiation

ABSTRACT

The Amazon forests play an integral role in the global carbon cycle and have a substantial impact on Earth's climate. However, it is increasingly susceptible to the effects of prolonged droughts, exacerbated by climate change and human activities. This vulnerability underscores the importance of understanding the forests' reaction to such environmental stressors. Despite their significance, comprehensive cross-comparisons of the climate and vegetation responses during the 2005, 2010, and 2015/2016 drought episodes are not well-established. Here we utilize a range of gridded vegetation and climate datasets—including leaf area index (LAI), solar-induced chlorophyll fluorescence (SIF), enhanced vegetation index (EVI), vegetation optical depth (VOD), self-calibrating Palmer drought severity index (scPDSI), precipitation (P), land surface temperature (LST), and photosynthetically active radiation (PAR)—to thoroughly assess the climate and vegetation response to these three drought events. Our findings reveal that the extent of drought inhibition in the Amazon forests was 74.7 % in 2015, increasing to 81.3 % in 2016, a significant escalation from 49.6 % in 2005 and 57.7 % in 2010. The effects of these three droughts on vegetation varied in both physiological and structural aspects. The Amazon forests' photosynthetic activity, greenness, and leaf area experienced comparable suppression in 2010 and 2015/2016 droughts. However, canopy water content exhibited more extensive and severe impacts during the 2015/2016 drought. Our findings indicate that varying sensitivities to water deficit and solar radiation lead to diverse spatial patterns and intensities of vegetation response, highlighting the complex dynamics of the Amazon forests under drought stress.

1. Introduction

The Amazon basin holds a critical position in global carbon and water cycles, accounting for nearly 50 % of the tropical forest carbon stocks. It is renowned as the most productive and biodiverse terrestrial ecosystem (Qin et al., 2021; Saatchi et al., 2011). Recent studies indicate a potential shift in the Amazon forests from being a carbon sink to a carbon source (Aragao et al., 2018; Brienen et al., 2015). Droughts are increasingly acknowledged as a critical factor regulating the short-term variability and long-term trend of carbon fluxes and stocks (Yang et al., 2018b). The projected increase in droughts' frequency and severity highlights the importance of investigating the impacts of droughts on Amazon forests (Dai, 2013; Lewis et al., 2011; Zhou et al., 2019).

The responses of tropical forests (especially Amazon forests) to droughts are not fully understood, presenting significant knowledge gaps in both observational and modeling studies. Historically, research has shown that droughts can lead to changes in forest structure and function, impacting tree mortality (Phillips et al., 2010), species composition (Engelbrecht et al., 2007), and carbon sequestration capabilities (Doughty et al., 2015). Field observations have provided

* Corresponding author at: Chongqing Jinfo Mountain Karst Ecosystem National Observation and Research Station, School of Geographical Sciences, Southwest University, Chongqing 400715, China.
E-mail address: liyao7@swu.edu.cn (Y. Li).

https://doi.org/10.1016/j.agrformet.2024.110051
Received 26 January 2024; Received in revised form 23 April 2024; Accepted 6 May 2024
Available online 15 May 2024

valuable insights into the immediate effects of drought on tropical forest ecosystems (Bennett et al., 2023). However, the lack of abundant *in situ* observations hinders a comprehensive understanding of the Amazon rainforest ecosystem (Atkinson et al., 2011). On the modeling front, efforts have been made to incorporate drought responses into ecosystem and climate models. Yet, significant gaps remain, particularly in accurately simulating the complex interactions between climate variability, forest dynamics, and biogeochemical cycles (Huntingford et al., 2013). Models often struggle to represent the diversity of tree species and their varying responses to drought, leading to uncertainties in predictions (Koch et al., 2021). Satellite observations have complemented these findings by offering a broader perspective on changes in forest canopy cover and biomass over larger areas and longer time scales (Atkinson et al., 2011; Xie et al., 2022).

Over the last two decades, the Amazon basin has experienced three significant drought extremes in 2005, 2010, and 2015/2016, leading to a profound impact on the global carbon cycle (Panisset et al., 2018). These droughts varied not only in duration but also in their underlying mechanisms. The 2005 and 2010 events were short-term droughts, each lasting less than three months, while the 2015/2016 event was a prolonged period of aridity, extending over six months (Jimenez-Munoz et al., 2016; Lewis et al., 2011; Marengo et al., 2008). The effects of each drought event on the Amazon forests have been thoroughly investigated (Anderson et al., 2010; Phillips et al., 2009; Saleska et al., 2007; Samanta et al., 2010; Wigneron et al., 2020). However, comprehensive cross-comparisons of these three droughts and their cumulative impacts on the forests remain unexplored (Anderegg et al., 2020). This absence of comparative analysis creates a significant gap in our understanding of the forests' sensitivity and resilience to varying drought patterns, particularly in the context of climate change (Shi et al., 2019; Wigneron et al., 2020). Addressing this gap is crucial for a more nuanced understanding of Amazon's response to environmental stressors. Moreover, the effects of these three extreme droughts on vegetation manifest differently, influencing factors such as photosynthetic activity (Koren et al., 2018), greenness (Anderson et al., 2010), biomass (Chen et al., 2019), and the capability for carbon sequestration (Doughty et al., 2015). Vegetation responses to drought conditions can vary significantly, both physiologically and structurally, across different levels from individual leaves to entire canopies (Zhang et al., 2013). Satellite remote sensing offers a comprehensive way to assess the drought impacts on vegetation across various scales (Asner and Alencar, 2010; Atkinson et al., 2011; Huete et al., 2006). Such satellite-based measurements enable a detailed evaluation of vegetation response to these extreme drought events, providing consistent temporal and spatial insights (Jiao et al., 2021; Zhou et al., 2014).

This study aims to comprehensively evaluate the impacts of the three extreme droughts on the Amazon forests, focusing on both physiological and structural aspects. To this end, we cross-compared the dynamics of Amazon forests during 2005, 2010, and 2015/2016 drought periods, utilizing a range of vegetation and climate related variables, including satellite-based leaf area index (LAI), solar-induced chlorophyll fluorescence (SIF), enhanced vegetation index (EVI), vegetation optical depth (VOD), land surface temperature (LST), photosynthetically active radiation (PAR), gridded self-calibrating Palmer drought severity index (scPDSI), and precipitation (P). Our objects are to 1) comprehensively quantify the variations in precipitation, temperature, radiation, and water balance anomalies across the three major drought events and 2) assess the impacts of these droughts on vegetation greenness, photosynthesis, canopy structure, and canopy water content of the Amazon forests.

2. Data and methods

2.1. Study area

The Amazon basin (18°S-8°N, 80°W-45°W) encompasses an area of ~6.3 million km^2 (Fig. 1). In this study, we focused on the evergreen broadleaf forest (EBF) regions, which account for 83.3 % of the basin according to the MODIS land cover data (MCD12C1.006). We utilized the MODIS land cover product from 2002 to 2018 to delineate the study area. Specifically, we selected the EBF category, identified by the LAI scheme with a value of 5, from each year's dataset. We then extracted the consistently overlapping regions across all selected years to define our study area. Our analysis is centered on the selected forest areas within the Amazon basin to evaluate the forests' resistance and response to droughts. Savannas and Grasslands were excluded due to their susceptibility to human activities.

2.2. Datasets

The datasets used in this study are summarized in Table 1. We selected the gridded scPDSI, P, LST, and PAR as key climate indicators to delineate the differences in water balance, rainfall, temperature, and radiation among the three drought events. The scPDSI dataset, employing the Penman-Monteith parameterization for the potential evapotranspiration calculation, has been extensively used to assess ecosystem water balance and drought conditions (Blunden and Arndt, 2020; van der Schrier et al., 2013). This dataset, originally at a 0.5° spatial resolution from 2000 to 2019, was resampled to a finer 0.05° resolution. To assess the water deficit during the droughts, we used precipitation data collected by the Tropical Rainfall Measuring Mission (TRMM, 3B43 Version 7) at a 0.25° spatial resolution from 2000 to 2019. This dataset was subjected to the same spatial resampling procedure to match the 0.05° resolution. Daytime LST data, derived from Collection 6 (C6) Aqua MODIS (MYD11C3) product from 2002 to 2019, were used to quantify temperature variations associated with vegetation and other climatic factors (Wan et al., 2015). The selection of Aqua MYD11C3 over Terra MOD11C3 was due to the pronounced distinction between vegetation and non-vegetation around 1:30 pm (Zhou et al., 2014). Additionally, we adopted monthly downward surface PAR values from Clouds and the Earth's Radiant Energy System (CERES, SYN1-deg_L3) at a 1° resolution between 2000 and 2019. The total incident all-sky PAR values were calculated by integrating direct and diffuse PAR fluxes (Rutan et al., 2015). Similar to the other datasets, the PAR data underwent spatial resampling to achieve the standard 0.05° resolution.

Satellite-based LAI, SIF, EVI, and VOD measurements were employed to represent canopy structure, vegetation photosynthesis, greenness, and canopy water content, respectively. LAI data were sourced from the Terra and Aqua MODIS LAI products (MOD15A2H and MYD15A2H) from 2000 to 2019 (Myneni et al., 2015a). These LAI datasets provide 8-day composite values with a 500 m global coverage. Following the method outlined by Chen et al. (2019), rigorous data quality control was

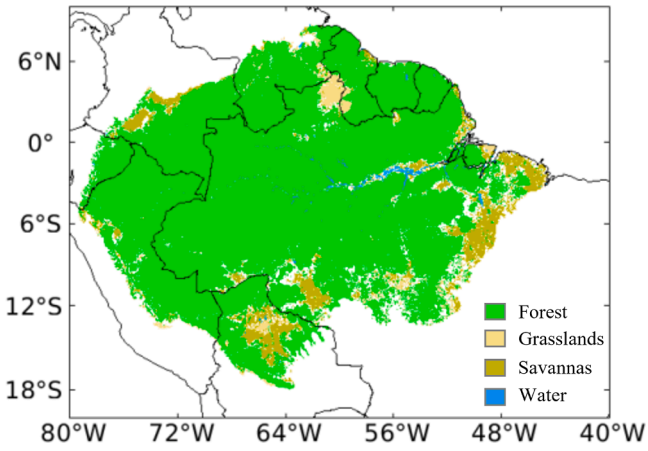

Fig. 1. Distribution of evergreen broadleaf forest (EBF) over the Amazon Basin based on the MODIS land cover data (MCD12C1.006).

Table 1
Overview of the meteorological and vegetation datasets used in the study.

Dataset	Products/Sensor	Spatial resolution	Temporal resolution	Period	Refs.
Land Cover	MCD12C1.006	0.05 °	yearly	2002–2018	Friedl and Sulla-Menashe (2015)
Drought Index	scPDSI, CRU TS 4.05	0.5 °	monthly	2000–2019	van der Schrier et al. (2013)
Precipitation	TRMM, 3B43 V7	0.25 °	monthly	2000–2019	Huffman et al. (2007)
LST	MYD11C3	0.05 °	monthly	2002–2019	Wan et al. (2015)
PAR	CERES, SYN1deg_L3	1 °	monthly	2000–2019	Doelling et al. (2016)
LAI	MOD15, MYD15	0.05 °	8-day	2000–2019	Myneni et al. (2015b)
SIF	OCO-2	0.05 °	4-day	2000–2018	Zhang et al. (2018)
EVI	MCD19A1 v006	0.05 °	8-day	2000–2017	Lyapustin et al. (2012)
VOD	VODCA Ku-band	0.25 °	daily	2000–2017	Moesinger et al. (2020)

implemented to achieve clean 16-day composite 0.05° LAI values. Subsequently, these 16-day values were composited into monthly datasets by weighing the days within each month. The spatially contiguous SIF (CSIF) dataset was provided by Zhang et al. (2018) at moderate resolutions (0.05° and 4-day) during the MODIS era. The 4-day CSIF dataset was then processed into monthly observations according to the day of year (DOY). The EVI dataset was derived using multi-angle implementation of atmospheric correction (MAIAC) MODIS land surface bidirectional reflectance factor (BRF) daily L2G global data (MCD19A1 v006) from 2000 to 2017 (Lyapustin et al., 2012). The MAIAC EVI products underwent stringent atmosphere, aerosol, and cloud corrections, along with bidirectional reflection distribution function (BRDF) correction (Guan et al., 2015; Lyapustin et al., 2012). In this way, the majority of artifacts in the MAIAC dataset were effectively removed. The global long-term microwave vegetation optical depth climate archive (VODCA) Ku-band (~19 GHz) dataset between 2000 and 2017 was obtained from Moesinger et al. (2020). This daily VOD dataset was aggregated into monthly data, corresponding to the DOY of each year. A uniform spatial resampling procedure was applied to the VOD data to obtain a consistent 0.05° dataset.

2.3. Methods

To assess the response of vegetation and climate variables to drought effects, we computed the standardized anomaly (SA) for each variable. The SA value was calculated using Eq. (1), where the multi-year average of valid monthly values from non-drought years served as the baseline. The years 2005, 2010, 2015, and 2016 were identified as drought years, with the remaining years from 2000 to 2019 serving as baseline years.

$$SA = \frac{V_{y,m} - \overline{V_m}}{\sigma} \quad (1)$$

where SA denotes the standardized anomaly, V represents the value of the variables (scPDSI, P, LST, PAR, LAI, SIF, EVI, and VOD), y stands for the year (ranging from 2000 to 2019), m is the month (Jan, Feb, …, Dec), $\overline{V_m}$ is the average value of the baseline years for month m, and σ is the standard deviation (SD) of the baseline values. To categorize the drought severity levels, the following thresholds were applied: incipient ($-1 < SA < -0.5$), slight ($-2 < SA < -1$), moderate ($-3 < SA < -2$), severe ($-4 < SA < -3$), and extreme ($SA < -4$). Note that LST and PAR used the corresponding positive anomalies. The threshold divisions were based on a synthesis of criteria from previous studies (van der Schrier et al., 2013).

The SA of the monthly gridded scPDSI data (SA_{scPDSI}) was utilized to assess the spatial distribution of duration and severity for the three drought episodes. To mitigate the impact of short-term variations, such as an abnormally wet month interrupting a prolonged dry period, we applied a three-month moving window to smooth the monthly SA_{scPDSI} data for each grid cell (Saft et al., 2015). Following the protocols established by Lewis et al. (2011) and Yang et al. (2018a), we set a threshold value of −1 to determine the onset and termination of each drought event. The onset of drought was identified when the SA_{scPDSI} value first dropped below −1 in a drought year, while the end was marked when the value rose above the threshold (Li et al., 2019). The drought duration for each grid cell was calculated by measuring the time span between the start and end months. Moreover, to assess the severity of each drought at the grid cell level, we computed the average SA_{scPDSI} value throughout the drought duration. On a regional scale, the extent of the area affected within the Amazon forests was analyzed by counting the number of grid cells where the SA_{scPDSI} value fell below the threshold of −1 during the drought episodes. This approach allows for a quantitative evaluation of the regional severity of the droughts.

3. Results and discussion

3.1. Cross-comparison of climate response to the three drought events

From the meteorological perspective, the 2015/2016 drought emerged as the most severe event in terms of intensity, duration, and spatial extent at both the grid and basin scales, surpassing the 2005 and 2010 drought events that were relatively shorter and less severe (Figs. 2). During the 2015/2016 drought, a substantial 74.7 % of the area experienced drought conditions ($SA_{scPDSI} < -1$) in 2015, escalating to 81.3 % in 2016. Notably, 30.8 % of the forest area suffered moderate to extreme drought ($SA_{scPDSI} < -2$) in 2016, marking the highest drought-affected rate over the last two decades. This drought event persisted into 2017 and reverted to pre-drought levels by 2018. In contrast, the 2005 and 2010 drought events had a smaller impact, with 49.6 % of the forest area affected in 2005 and 57.7 % in 2010 ($SA_{scPDSI} < -1$), followed by a rapid return to pre-drought conditions (Fig. 2).

Regarding the driving factors behind these droughts, the 2015/2016 event was distinguished by significantly reduced precipitation (decreases of 12.7 % and 9.9 %), notably high temperatures (increases of 0.4 °C and 0.6 °C), and considerably intense radiation (increases of 1.2 % and 0.9 %) compared to the baseline of non-drought years. In contrast, the 2005 drought experienced a modest decline in precipitation (−3.2 %), a minor increase in temperature (+0.2 °C), and a noticeable decrease in radiation (−1.1 %). The 2010 drought, on the other hand, was characterized by a substantial reduction in precipitation (−8.3 %), a remarkable rise in temperature (+0.5 °C), and a moderate increase in radiation (+0.8 %) (Fig. 3).

Spatially, the 2015/2016 drought impacted a more extensive area of the Amazon forests compared to the droughts of 2005 and 2010. In 2005, the drought affected 49.6 % of the forest area ($SA_{scPDSI} < -1$) (Fig. 4a), and 3.9 % of the forests experienced a year-long drought (i.e., duration = 12 months), mainly in the central and southern regions (Fig. 4b). The 2010 drought was more widespread, impacting 57.7 % of the forests ($SA_{scPDSI} < -1$), particularly in the western, southeastern, and northern edges (Fig. 4c), but only 1.2 % experienced a year-long drought (Fig. 4d). The 2015/2016 drought, the most severe in the past two decades, astonishingly affected 74.7 % (2015) and 81.3 % (2016) of the forest area ($SA_{scPDSI} < -1$), nearly encompassing the entire Amazon forest (Fig. 4e and 4 g). Additionally, 8.2 % (primarily in central and northern regions) in 2015 and 32.7 % (across the study area) in 2016 endured a year-long drought (Fig. 4f and 4h). More concerning is that 4.9 % of the forests suffered from drought for up to 24 months, although

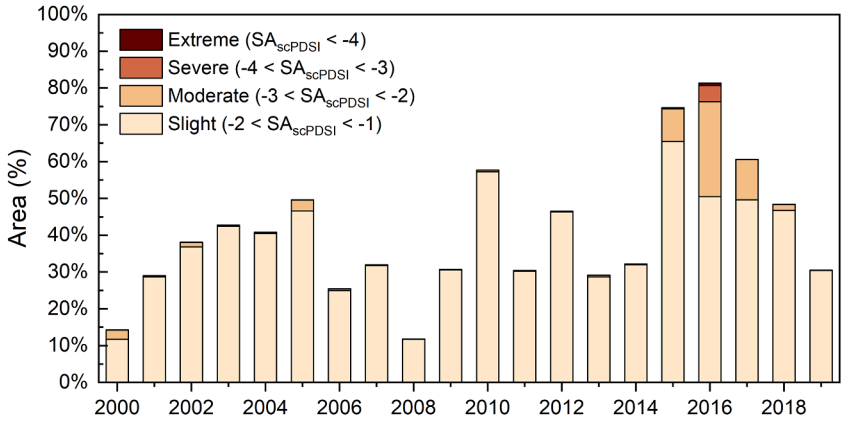

Fig. 2. Statistical analysis of areas (compared to the total study area) affected by various degrees of droughts from 2000 to 2019.

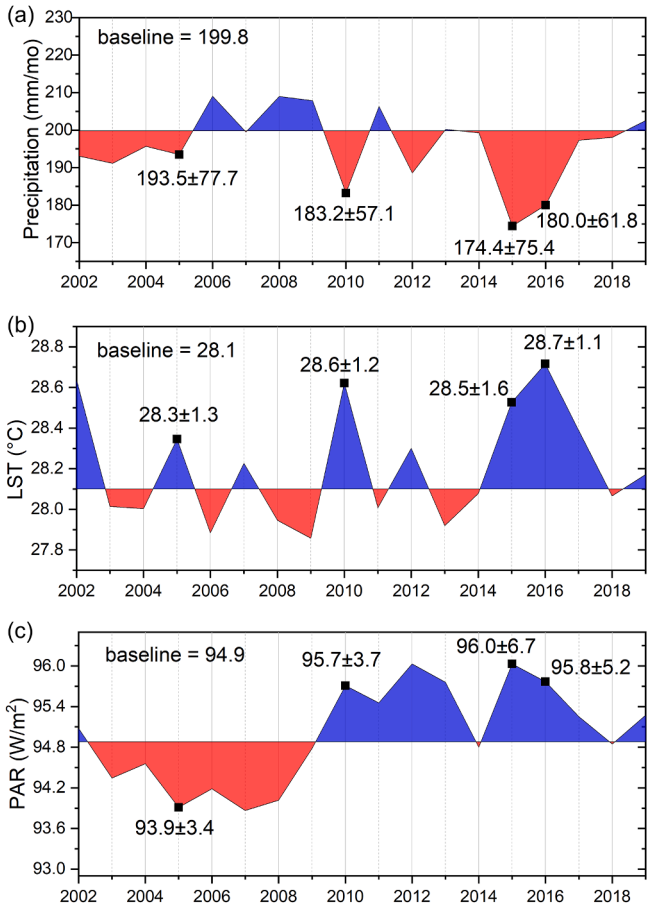

Fig. 3. Annual average of (a) precipitation, (b) land surface temperature (LST), and (c) photosynthetically active radiation (PAR) in the Amazon forests from 2002 to 2019. Annual mean and the corresponding standard deviation values for the drought years 2005, 2010, 2015, and 2016 are highlighted and annotated. Baseline levels were calculated as average values from 2002 to 2019, excluding these four drought years.

they did not exhibit a clear spatial pattern.

Temporally, the 2005 and 2010 droughts primarily occurred during the dry season (July-September), whereas the 2015/2016 drought spanned from the late dry season into the wet season (September-May) across the Amazon forests. This variation in timing, as shown in Fig. 5, reflects the different meteorological factors driving each drought event. In the 2005 drought, drought conditions (scPDSI < -1) began in June, peaking in July (21.2 %), followed by August (20.7 %) and September (19.8 %) according to the scPDSI data (Fig. 5a) when the largest area experienced a precipitation deficit (Fig. 5b). This peak period of July to September aligns with the findings of Marengo et al. (2008). The 2005 drought event was caused by the combination of El Niño and a dry spell attributable to a warm subtropical North Atlantic Ocean (Zeng et al., 2008). Unlike the Pacific influence, which is usually limited to the wet season, the impact of the 2005 Atlantic event was focused on the Amazon dry season when its hydroecosystem was particularly vulnerable. The 2010 drought, influenced by warmer sea surface temperature (SST) in the Atlantic Ocean (Jimenez et al., 2018), saw 18.7 % (September) and 17.8 % (October) of the area experience drought (Fig. 5a). An additional peak occurred in the wet season (19.4 % in March), attributed to a moderate to strong positive El Niño Southern Oscillation (ENSO) in late 2009, exacerbating drought conditions in the 2010 dry season (Jimenez et al., 2018). The 2015/2016 drought, starting in September 2015 (29.3 %) and peaking in January 2016 (46.2 %), coincided with P (Fig. 5b) and LST (Fig. 5c). Although P and LST returned to normal levels within 2016, the drought's impact persisted until the end of 2017 according to scPDSI. The extended period of low precipitation and extremely high temperatures resulted in the most severe drought since 2000 (Jimenez-Munoz et al., 2016). Prior to 2015, increases in SST in the equatorial region had raised concerns about intensified ENSO events and shifts in the intertropical convergence zone, which could potentially alter the precipitation patterns in the Amazon. This could lead to longer dry seasons and more frequent severe droughts (Fu et al., 2013; Hilker et al., 2014).

3.2. Cross-comparison of vegetation response to the three drought events

The responses of Amazon forests to 2005, 2010, and 2015/2016 droughts, as indicated by four vegetation parameters, can be categorized into two distinct cases. First, canopy water content represented by VOD showed that the 2015/2016 drought had the most severe and widespread impacts, aligning with climate observations. Approximately 49 % of the Amazon forests experienced canopy water suppression (SA$_{VOD}$ < -1) during this period, 18.3 % and 24.9 % more than in 2005 and 2010, respectively (Figs. 6 and 7). Conversely, the severities of the three droughts appeared comparable when analyzed using three optical variables, including LAI, SIF, and EVI (Figs. 6 and 7). In 2015/2016, an anomalously low level of photosynthetic activity (SA$_{SIF}$ < -1) affected over 22.2 % of the Amazon forests, in contrast to 12.9 % in 2005 and 24.5 % in 2010 (Figs. 6 and 7). Notable anomalies in greenness (SA$_{EVI}$ < -1) were observed in over 25.1 % of the study area in 2015/2016, in contrast to 15.6 % in 2005 and 21.8 % in 2010 (Figs. 6 and 7). The proportions of the Amazon forests with significant reductions in leaf area (SA$_{LAI}$ < -1) were relatively similar (11.0 %, 15.2 %, and 11.6 %, in 2005, 2010, and 2015/2016, respectively) (Figs. 6 and 7).

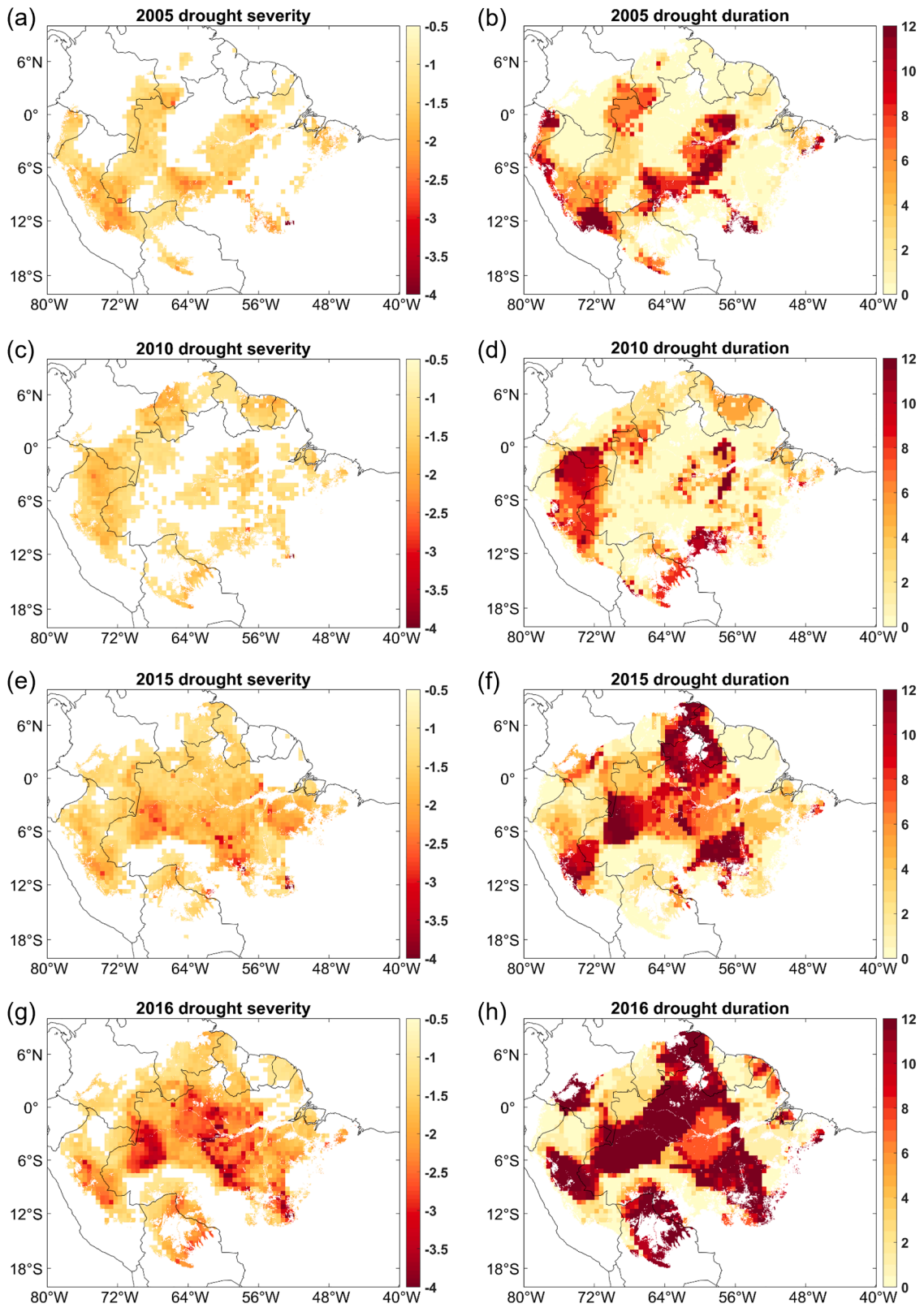

Fig. 4. Spatial distribution of drought severity (inferred by SA_{scPDSI}) and duration ($SA_{scPDSI} < -1$) in 2005, 2010, 2015, and 2016.

While the severity and duration of vegetation responses varied across each drought, the spatial distributions of the affected areas, as indicated by four vegetation parameters, exhibited similar patterns (Fig. 6). The 2005 drought had a relatively limited impact, mainly confined to the southern and southwestern regions of the Amazon forests. This drought was identified as the least severe with the shortest duration among the three events (Figs. 2 and 4). All four vegetation parameters showed a nearly neutral response to the 2005 drought, consistent with findings by Samanta et al. (2010) that reported no significant large-scale greening or browning of the Amazon forests during the 2005 dry season (Fig. 6). This

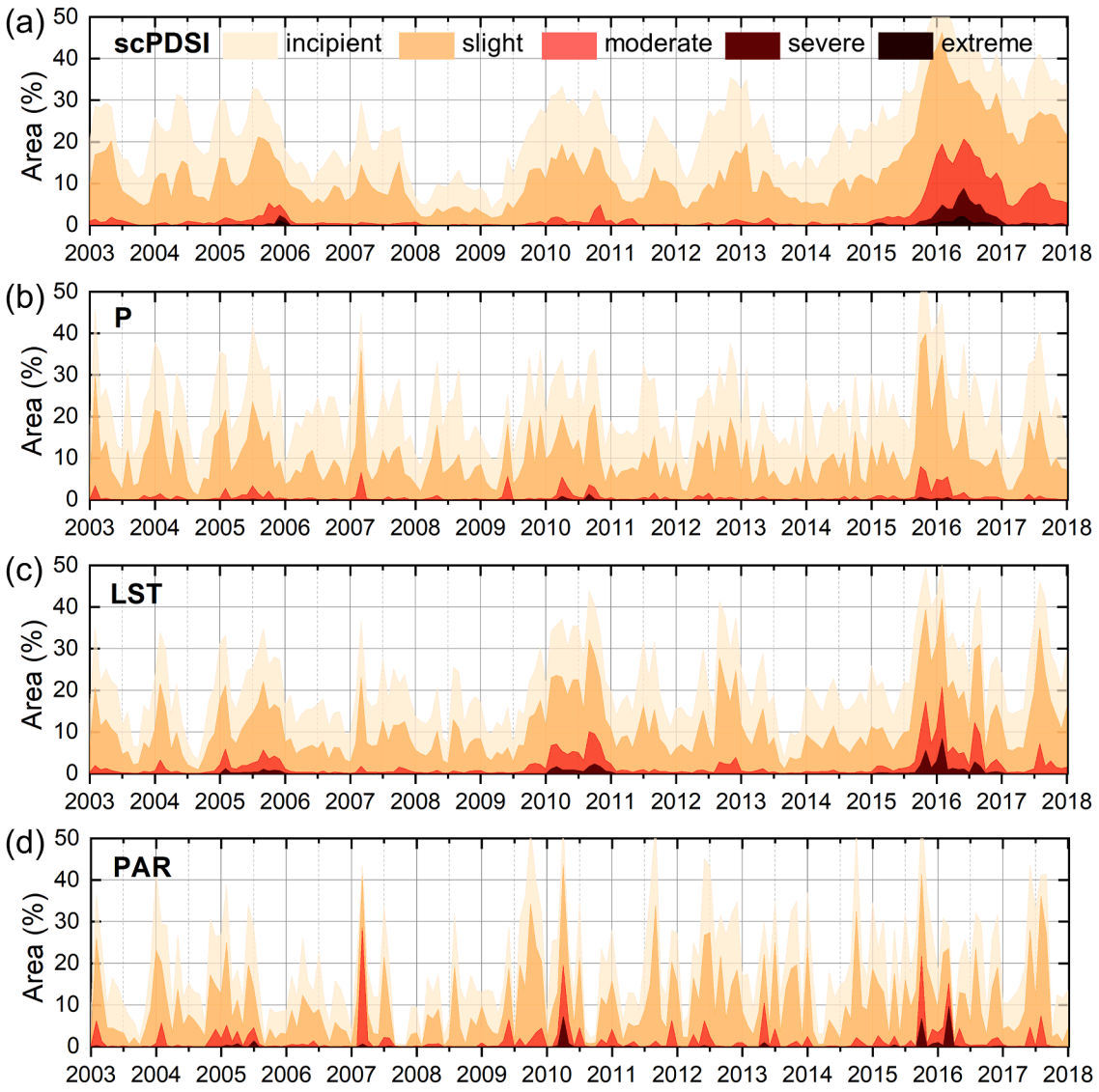

Fig. 5. Monthly statistics of Amazon forests area under different anomaly levels (incipient, slight, moderate, severe, and extreme) for four meteorological parameters: (a) self-calibrating Palmer drought severity index (scPDSI), (b) precipitation (P), (c) land surface temperature (LST), and (d) photosynthetically active radiation (PAR) from 2003 to 2017.

observation is supported by statistical analyses of the anomalies in the four vegetation variables (Fig. 7**).** In comparison, the 2010 drought had a more substantial and widespread effect on the forests, particularly in the peripheral regions of the basin, across all four parameters (Fig. 6). This finding agrees well with the previous studies (Bi et al., 2016; Lewis et al., 2011; Xu et al., 2011). The 2015/2016 drought presented diverse results according to these four satellite-based vegetation variables (Fig. 6). Approximately 10 % of the leaf area experienced effects, while over 20 % of the forests saw a decrease in photosynthesis, and as much as 25 % showed a reduction in greenness. Meanwhile, nearly 50 % of the Amazon forests displayed a shortfall in canopy water content.

SIF has proven to be more sensitive to environment-induced photosynthetic variations than conventional vegetation indices, which mainly focus on canopy greenness and chlorophyll content. This heightened sensitivity is due to SIF's direct physiological connection with photosynthetic activity (Daumard et al., 2010; Li et al., 2018; Qian et al., 2019; Yang et al., 2018a; Yoshida et al., 2015). During drought periods, the spatial correlation between SIF and PAR was relatively higher than other vegetation indicators (Table 2). From the aspect of SIF, the 2010 drought was more extensive and severe in terms of spatial coverage than the 2005 drought (Fig. 6). Compared to the 2010 drought, the 2015/2016 drought experienced a similar proportion of the area affected by slight to moderate conditions. However, there was a noticeable increase in the area and duration of severe anomalies during the 2015/2016 event.

The EVI, rather than the normalized difference vegetation index (NDVI), is typically preferred for monitoring vegetation greenness in tropical rainforests during droughts, as NDVI data often become saturated in these environments (Saleska et al., 2007). EVI derived from the MAIAC product is deemed more accurate due to its less conservative cloud detection algorithm than the standard Collection 5 and Collection 6 MODIS products (Hilker et al., 2014). Our findings reveal that the proportion of areas experiencing a slight to extreme EVI anomaly ($SA_{EVI} < -1$) during the 2010 dry season (Jul-Aug-Sep, JAS) was 20.4 %, which was higher than the 13.2 % observed in 2005, aligning with the observations in Lewis et al. (2011) and Xu et al. (2011). Additionally, compared to P and PAR, LST had a higher spatial correlation with EVI (Table 2), suggesting that LST significantly influences vegetation greenness.

LAI showed the least sensitivity to droughts among the vegetation parameters (Table 2). Influenced by leaf flushing and abscission, LAI exhibited notable seasonal phenology in Amazon forests (Myneni et al.,

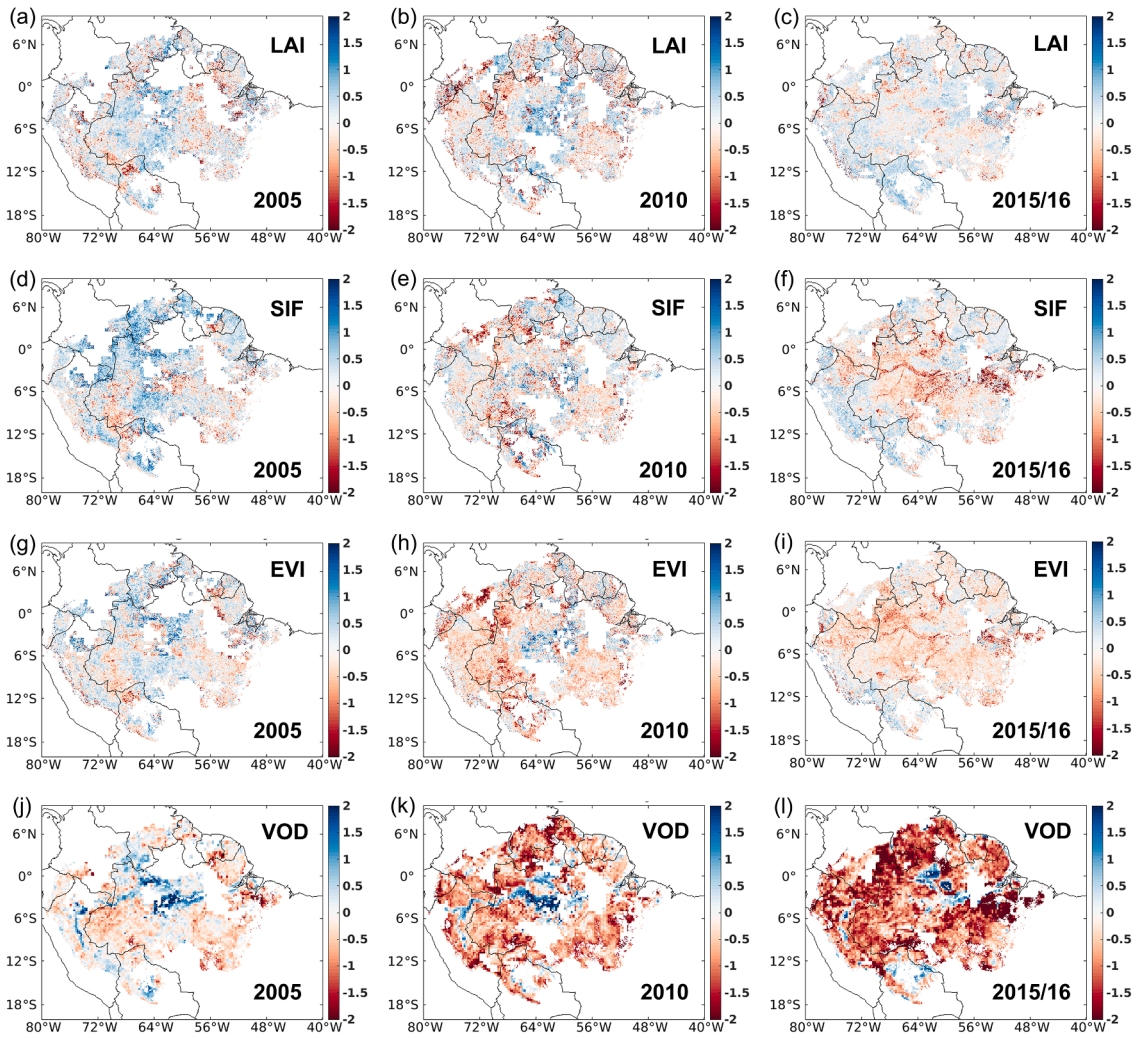

Fig. 6. Spatial distribution of standardized anomaly in (a-c) leaf area index (LAI), (d-f) solar-induced chlorophyll fluorescence (SIF), (g-i) enhanced vegetation index (EVI), and (j-l) vegetation optical depth (VOD) during the 2005, 2010, and 2015/2016 drought events.

2007; Samanta et al., 2012), and there was not a significant increase in tree mortality during the 2015/2016 drought (Bennett et al., 2021). Moreover, the spatial correlation between LAI and P was very weak during these four drought periods (Table 2). This weak correlation partially accounts for LAI's relative insensitivity to drought conditions, suggesting that factors other than precipitation significantly influence LAI dynamics in the Amazon forests.

3.3. *Divergent responses across satellite-based measurements*

The divergent results between VOD and other vegetation indicators for the 2015/2016 drought might be attributed to two reasons. First, an increase in at-surface solar radiation during this period potentially enhanced vegetation photosynthesis. Solar radiation showed a significant rise during the water deficit months of 2015 and 2016 (Fig. 3). Higher levels of absorbed solar radiation could partially counteract the adverse effects of water stress on Amazon forests' photosynthesis during drought conditions (Green et al., 2020; Li et al., 2018; Yan et al., 2019). It has been reported that solar radiation plays a crucial role in forest photosynthesis and leaf flushing during dry periods (Bi et al., 2015; Doughty et al., 2019; Myneni et al., 2007). The second reason pertains to the deep roots of evergreen rainforests that are more resistant to water deficits (Bennett et al., 2021). These forests with deep roots can sustain evapotranspiration by drawing water from soil depths exceeding eight meters for up to five months during dry periods (Giardina et al., 2018; Nepstad et al., 1994). The microwave variable (VOD) is sensitive to changes in the soil's dielectric properties due to water content fluctuations (Zhang et al., 2013), a measured feature not detectable by optical sensors. Hence, while optical parameters (LAI, SIF, and EVI) effectively capture the impact of solar radiation on seasonal phenology, they are susceptible to weather and atmospheric conditions. In contrast, canopy water content, as measured by microwave sensor data (VOD), can provide earlier and more pronounced water stress indicators due to its superior penetration ability (Fig. 7).

The diverse responses of vegetation indices to droughts align with understanding plant physiological responses to water stress. Droughts can trigger stomatal closure, thereby impeding the photosynthetic process. When soil moisture decreases due to insufficient rainfall, plants tend to respond by closing the stomata. This response can cause a temporary reduction in photosynthesis, which might quickly recover or result in a delayed onset of the subsequent wet season (Shi et al., 2019). Prolonged droughts may lead to a reduction in enzymatic activity within plants (Zhang et al., 2013), and in extreme cases, sustained drought stress can affect the leaf area of canopies, potentially culminating in forest die-offs (Phillips et al., 2009, 2010). Thus, areas impacted by severe and extreme droughts may indicate forest degradation, with severe anomalies predominantly observed in drought years (i.e., 2005, 2010, 2015, and 2016). The extent of areas with moderate anomalies was notably larger during drought years compared to non-drought years. However, it remains challenging to distinguish drought periods based on

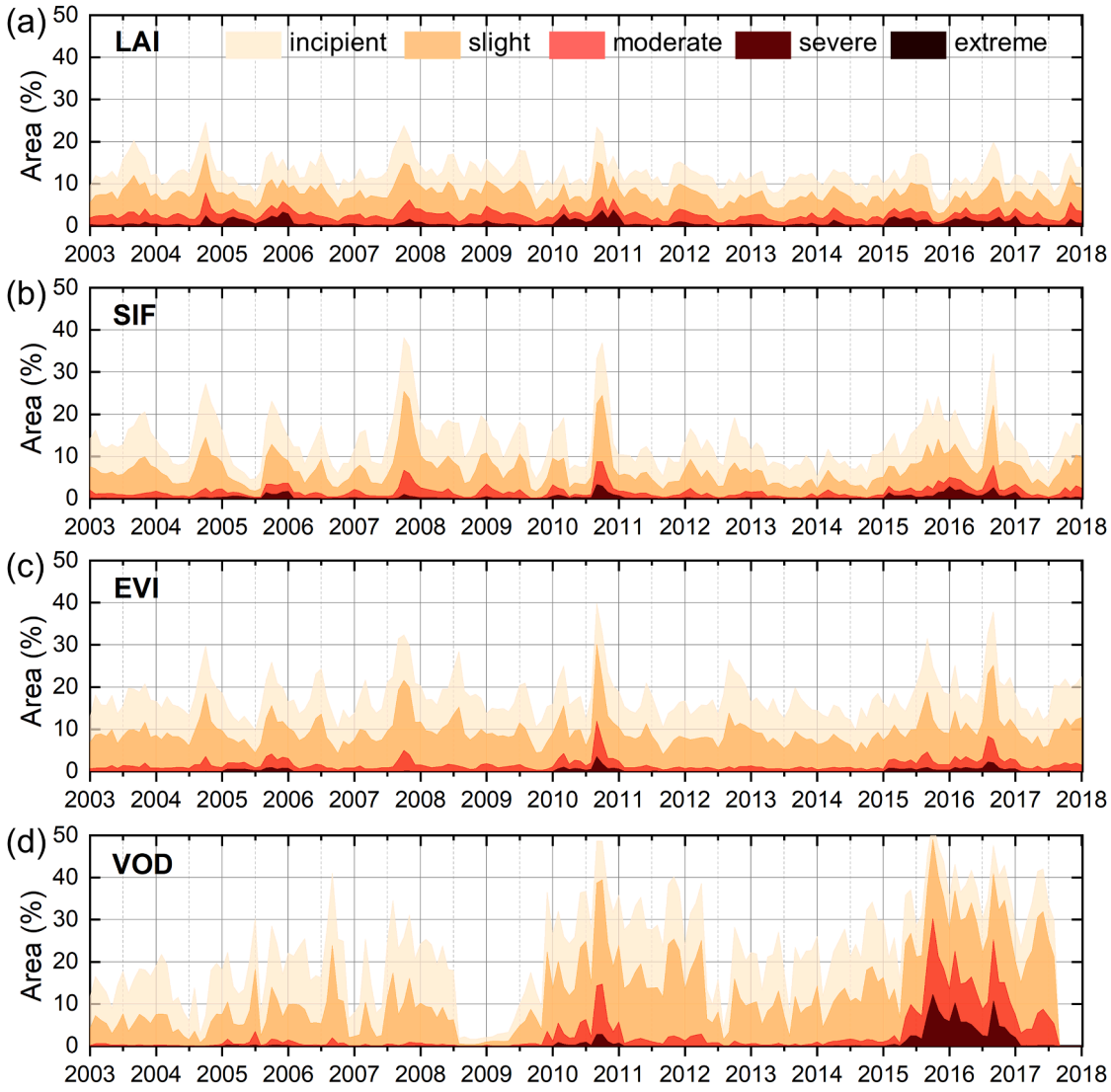

Fig. 7. Monthly statistics of Amazon forest areas under different drought levels (incipient, slight, moderate, severe, and extreme) based on four vegetation parameters: (a) leaf area index (LAI), (b) solar-induced chlorophyll fluorescence (SIF), (c) enhanced vegetation index (EVI), and (d) vegetation optical depth (VOD) from 2003 to 2017.

Table 2
Pearson correlation coefficient (r) for spatial standardized anomaly data between four vegetation parameters and three climate parameters during the four drought quarter periods (2005 JAS, 2010 JAS, 2015 SON, and 2016 DJF).

		LAI	SIF	EVI	VOD
2005	**P**	0.0009	0.0179	0.0039	0.0262
JAS	**LST**	-0.1381	-0.1938	-0.2266	-0.1307
	PAR	0.0388	0.0548	0.0232	-0.0488
2010	**P**	0.0153	0.0274	0.0737	-0.1549
JAS	**LST**	-0.0872	-0.181	-0.1684	-0.0089
	PAR	0.0836	0.0631	0.1412	-0.0962
2015	**P**	0.0311	0.0995	0.0731	0.0833
SON	**LST**	-0.0876	-0.2585	-0.195	-0.2095
	PAR	0.112	0.1119	0.0515	-0.0846
2016	**P**	-0.0306	0.0532	N/A	0.0709
DJF	**LST**	0.0116	-0.0716	N/A	-0.0862
	PAR	0.1709	0.2483	N/A	N/A

Note that the r values are illustrated using a red-green diverging color scheme, where red indicates a positive correlation, and green denotes a negative correlation. The intensity of the color corresponds to the absolute value of r. "N/A" signifies that the results did not satisfy the significance test ($p < 0.001$).

incipient and slight anomalies (Fig. 7).

In tropical rainforests, sunlight is generally the dominant driver of photosynthesis (Huete et al., 2006; Myneni et al., 2007). These forests are considered more resistant to droughts due to their deep-root system. Since short-term vegetation growth is influenced by factors such as light (Smith et al., 2019), CO_2 fertilization (Zhu et al., 2016), and soil moisture (Saleska et al., 2007), moderate anomalies caused by precipitation deficits in the Amazon may recover more readily (Bi et al., 2015). There is a one- to two-month lag between water deficit and vegetation inhibition, attributed to the high soil water holding capacity in forests (Xiao et al., 2005). Even during the 2015/2016 event, significant vegetation suppression was not observed in the initial stages. A significant anomaly emerged during the dry season of 2016, coinciding with the end of the drought. This anomaly indicated a lagged response of the vegetation to the drought conditions (Fig. 7), consistent with findings that forests in the tropical Amazon showed little to no recovery in 2017 (Wigneron et al., 2020).

It is important to note that the findings of this study predominantly rely on satellite datasets, which inherently carry some degree of uncertainty (Galvão et al., 2011). To minimize these uncertainties, we meticulously selected satellite-based datasets renowned for their high quality. For instance, the MODIS C6 LAI dataset is recognized as one of the latest and most reliable products in this category. Furthermore, we integrated the MOD15 and MYD15 datasets, applying stringent quality control as Chen et al. (2019) outlined. Given the saturation issues of NDVI in dense forests, we opted for EVI in our study. The MAIAC EVI product, chosen for its accurate representation of vegetation greenness, effectively addresses concerns related to observational positioning (Bi et al., 2015). The MAIAC data undergo rigorous atmospheric, aerosol, and cloud corrections, in addition to BRDF adjustments (Guan et al., 2015; Lyapustin et al., 2012), significantly reducing the presence of artifacts and enhancing the overall data quality.

4. Conclusions

From a climate perspective, the 2015/2016 drought ranked as the most severe of the three major drought events since 2000. However, when evaluated from physiological and structural perspectives, the response of the Amazon forests to these droughts showed considerable variation. The 2005 drought was the least severe and had the shortest duration among the three. Compared to 2005, the Amazon forests experienced greater severity and a much broader effect during the 2010 drought. During the 2015/2016 drought, the patterns observed in optical satellite-based variables (such as leaf area, photosynthetic activity, and greenness) and microwave measurements (vegetation optical depth) diverged. The impact of the 2015/2016 drought, in terms of optical variables, was comparable to that of the 2010 drought. Yet, the canopy water content, as measured by microwave data, indicated more extensive and severe drought impacts in 2015/2016. This could be attributed to the reduced sunlight during this drought period and the capability of the deep-rooted, intact evergreen forests to extract water from deeper soil layers during prolonged droughts. Among the four vegetation parameters analyzed in this study, canopy water content was the most responsive to hydrologic stress, followed by photosynthetic activity and greenness, with leaf area being the least sensitive to drought conditions.

CRediT authorship contribution statement

Xiaojun She: Writing – original draft, Project administration, Methodology, Investigation, Funding acquisition, Formal analysis, Data curation, Conceptualization. **Yao Li:** Writing – review & editing, Project administration, Investigation, Funding acquisition, Formal analysis, Conceptualization. **Wenzhe Jiao:** Investigation, Conceptualization. **Yuanheng Sun:** Data curation. **Xiangnan Ni:** Data curation. **Zhenpeng Zuo:** Data curation. **Yuri Knyazikhin:** Writing – review & editing, Supervision, Resources, Investigation, Formal analysis, Data curation, Conceptualization. **Ranga B. Myneni:** Writing – review & editing, Supervision, Resources, Methodology, Investigation, Formal analysis, Data curation, Conceptualization.

Declaration of competing interest

The authors declare that they have no known competing financial interests or personal relationships that could have appeared to influence the work reported in this paper.

Data availability

Data will be made available on request.

Acknowledgments and Data

This work was supported by the National Natural Science Foundation of China (42001288, 42201349), China Scholarship Council (201806995081), and Southwest University Startup Fund for Scientific Scholars (SWU116083). The scPDSI data were available at https://crudata.uea.ac.uk/cru/data/drought/#global. TRMM (TMPA/3B43) precipitation data were downloaded at https://disc.gsfc.nasa.gov/datasets/TRMM_3B43_7/summary. LST data and LAI data were obtained through the online Data Pool at the NASA Land Processes Distributed Active Archive Center (LP DAAC), USGS/Earth Resources Observation and Science (EROS) Center (https://lpdaac.usgs.gov). CERES PAR data were collected from https://ceres.larc.nasa.gov/data. VOD data were available at https://zenodo.org/record/2575599#.YJhOmSj0mUm. We thank Dr. Yao Zhang for providing the CSIF dataset and Drs. Alexei Lyapustin and Yujie Wang for providing MAIAC VI data.

References

Anderegg, W.R.L., Trugman, A.T., Badgley, G., Konings, A.G., Shaw, J., 2020. Divergent forest sensitivity to repeated extreme droughts. Nat. Clim. Change. 10 (12), 1091–1095.
Anderson, L.O., et al., 2010. Remote sensing detection of droughts in Amazonian forest canopies. New Phytol. 187 (3), 733–750.
Aragao, L., et al., 2018. 21st Century drought-related fires counteract the decline of Amazon deforestation carbon emissions. Nat. Commun. 9 (1), 536.
Asner, G.P., Alencar, A., 2010. Drought impacts on the Amazon forest: the remote sensing perspective. New Phytol. 187 (3), 569–578.
Atkinson, P.M., Dash, J., Jeganathan, C., 2011. Amazon vegetation greenness as measured by satellite sensors over the last decade. Geophys. Res. Lett. 38 (19).
Bennett, A.C., et al., 2021. Resistance of African tropical forests to an extreme climate anomaly. Proc. Natl. Acad. Sci. U. S. A. 118 (21), e2003169118.
Bennett, A.C., et al., 2023. Sensitivity of South American tropical forests to an extreme climate anomaly. Nat. Clim. Change 13 (9), 967–974.
Bi, J., et al., 2015. Sunlight mediated seasonality in canopy structure and photosynthetic activity of Amazonian rainforests. Environ. Res. Lett. 10 (6), 064014.
Bi, J., et al., 2016. Amazon forests' response to droughts: a perspective from the MAIAC product. Remote Sens. 8 (4), 356.
Blunden, J., Arndt, D.S., 2020. State of the climate in 2019. Bull. Am. Meteorol. Soc. 101 (8), S1–S429.
Brienen, R.J., et al., 2015. Long-term decline of the Amazon carbon sink. Nature 519 (7543), 344–348.
Chen, C., et al., 2019. China and India lead in greening of the world through land-use management. Nat. Sustain. 2 (2), 122–129.
Dai, A., 2013. Increasing drought under global warming in observations and models. Nat. Clim. Change 3 (1), 52–58.
Daumard, F., et al., 2010. A field platform for continuous measurement of canopy fluorescence. IEEE Trans. Geosci. Remote Sens. 48 (9), 3358–3368.
Doelling, D.R., et al., 2016. Advances in geostationary-derived longwave fluxes for the CERES synoptic (SYN1deg) product. J. Atmos. Ocean. Technol. 33 (3), 503–521.
Doughty, C.E., et al., 2015. Drought impact on forest carbon dynamics and fluxes in Amazonia. Nature 519 (7541), 78–82.
Doughty, R., et al., 2019. TROPOMI reveals dry-season increase of solar-induced chlorophyll fluorescence in the Amazon forest. Proc. Natl. Acad. Sci. U. S. A. 116 (44), 22393–22398.
Engelbrecht, B.M., et al., 2007. Drought sensitivity shapes species distribution patterns in tropical forests. Nature 447 (7140), 80–82.

Friedl, M., Sulla-Menashe, D., 2015. MCD12C1 MODIS/Terra+Aqua Land Cover Type Yearly L3 Global 0.05Deg CMG V006. NASA EOSDIS Land Processes Distributed Active Archive Center.
Fu, R., et al., 2013. Increased dry-season length over southern Amazonia in recent decades and its implication for future climate projection. Proc. Natl. Acad. Sci. U. S. A. 110 (45), 18110–18115.
Galvão, L.S., et al., 2011. On intra-annual EVI variability in the dry season of tropical forest: a case study with MODIS and hyperspectral data. Remote Sens. Environ. 115 (9), 2350–2359.
Giardina, F., et al., 2018. Tall Amazonian forests are less sensitive to precipitation variability. Nat. Geosci. 11 (6), 405–409.
Green, J., Berry, J., Ciais, P., Zhang, Y., Gentine, P., 2020. Amazon rainforest photosynthesis increases in response to atmospheric dryness. Sci. Adv. 6 (47), eabb7232.
Guan, K., et al., 2015. Photosynthetic seasonality of global tropical forests constrained by hydroclimate. Nat. Geosci. 8 (4), 284–289.
Hilker, T., et al., 2014. Vegetation dynamics and rainfall sensitivity of the Amazon. Proc. Natl. Acad. Sci. U. S. A. 111 (45), 16041–16046.
Huete, A.R., et al., 2006. Amazon rainforests green-up with sunlight in dry season. Geophys. Res. Lett. 33 (6).
Huffman, G.J., et al., 2007. The TRMM multisatellite precipitation analysis (TMPA): quasi-global, multiyear, combined-sensor precipitation estimates at fine scales. J. Hydrometeorol. 8 (1), 38–55.
Huntingford, C., et al., 2013. Simulated resilience of tropical rainforests to CO2-induced climate change. Nat. Geosci. 6 (4), 268–273.
Jiao, W., Wang, L., McCabe, M.F., 2021. Multi-sensor remote sensing for drought characterization: current status, opportunities and a roadmap for the future. Remote Sens. Environ. 256, 112313.
Jimenez-Munoz, J.C., et al., 2016. Record-breaking warming and extreme drought in the Amazon rainforest during the course of El Nino 2015-2016. Sci. Rep. 6, 33130.
Jimenez, J.C., Libonati, R., Peres, L.F., 2018. Droughts over Amazonia in 2005, 2010, and 2015: a cloud cover perspective. Front. Earth. Sci. 6, 227.
Koch, A., Hubau, W., Lewis, S.L., 2021. Earth system models are not capturing present-day tropical forest carbon dynamics. Earths Future 9 (5).
Koren, G., et al., 2018. Widespread reduction in sun-induced fluorescence from the Amazon during the 2015/2016 El nino. Philos. Trans. R. Soc. Lond. B Biol. Sci. 373 (1760).
Lewis, S.L., Brando, P.M., Phillips, O.L., van der Heijden, G.M., Nepstad, D., 2011. The 2010 Amazon drought. Science 331 (6017), 554.
Li, X., et al., 2019. The impact of the 2009/2010 drought on vegetation growth and terrestrial carbon balance in Southwest China. Agric. For. Meteorol. 269, 239–248.
Li, X., Xiao, J., He, B., 2018. Higher absorbed solar radiation partly offset the negative effects of water stress on the photosynthesis of Amazon forests during the 2015 drought. Environ. Res. Lett. 13 (4), 044005.
Lyapustin, A.I., et al., 2012. Multi-angle implementation of atmospheric correction for MODIS (MAIAC): 3. Atmospheric correction. Remote Sens. Environ. 127, 385–393.
Marengo, J.A., et al., 2008. The drought of Amazonia in 2005. J. Clim. 21 (3), 495–516.
Moesinger, L., et al., 2020. The global long-term microwave vegetation optical depth climate archive (VODCA). Earth. Syst. Sci. Data 12 (1), 177–196.
Myneni, R., Knyazikhin, Y., Park, T., 2015a. MOD15A2H MODIS/Terra Leaf Area Index/FPAR 8-Day L4 Global 500m SIN Grid V006. NASA EOSDIS Land Processes Distributed Active Archive Center.
Myneni R., Knyazikhin Y. and Park T., 2015b. MYD15A2H MODIS/Aqua Leaf Area Index/FPAR 8-Day L4 Global 500m SIN Grid V006. NASA EOSDIS Land Processes Distributed Active Archive Center.
Myneni, R.B., et al., 2007. Large seasonal swings in leaf area of Amazon rainforests. Proc. Natl. Acad. Sci. 104 (12), 4820–4823.
Nepstad, D.C., et al., 1994. The role of deep roots in the hydrological and carbon cycles of Amazonian forests and pastures. Nature 372, 666–669.
Panisset, J.S., et al., 2018. Contrasting patterns of the extreme drought episodes of 2005, 2010 and 2015 in the Amazon Basin. Int. J. Climatol. 38 (2), 1096–1104.
Phillips, O.L., et al., 2009. Drought sensitivity of the Amazon rainforest. Science 323 (5919), 1344–1347.
Phillips, O.L., et al., 2010. Drought-mortality relationships for tropical forests. New. Phytol. 187 (3), 631–646.
Qian, X., Qiu, B., Zhang, Y., 2019. Widespread decline in vegetation photosynthesis in Southeast Asia due to the prolonged drought during the 2015/2016 El Niño. Remote Sens. 11 (8), 910.
Qin, Y., et al., 2021. Carbon loss from forest degradation exceeds that from deforestation in the Brazilian Amazon. Nat. Clim. Chang. 11 (5), 442–448.
Rutan, D.A., et al., 2015. CERES synoptic Product: methodology and validation of surface radiant flux. J. Atmos. Ocean. Technol. 32 (6), 1121–1143.
Saatchi, S.S., et al., 2011. Benchmark map of forest carbon stocks in tropical regions across three continents. Proc. Natl. Acad. Sci. U. S. A. 108 (24), 9899–9904.
Saft, M., Western, A.W., Zhang, L., Peel, M.C., Potter, N.J., 2015. The influence of multiyear drought on the annual rainfall-runoff relationship: an Australian perspective. Water Resour. Res. 51 (4), 2444–2463.
Saleska, S.R., Didan, K., Huete, A.R., Rocha, H.R.d., 2007. Amazon forests green-up during 2005 drought. Science 318 (5850), 612.
Samanta, A., et al., 2010. Amazon forests did not green-up during the 2005 drought. Geophys. Res. Lett. 37 (5).
Samanta, A., et al., 2012. Seasonal changes in leaf area of Amazon forests from leaf flushing and abscission. J. Geophys. Res. Biogeosciences 117 (G1).
Shi, M., et al., 2019. The 2005 Amazon drought legacy effect delayed the 2006 wet season onset. Geophys. Res. Lett. 46 (15), 9082–9090.
Smith, M.N., et al., 2019. Seasonal and drought-related changes in leaf area profiles depend on height and light environment in an Amazon forest. New Phytol. 222 (3), 1284–1297.
van der Schrier, G., Barichivich, J., Briffa, K.R., Jones, P.D., 2013. A scPDSI-based global data set of dry and wet spells for 1901-2009. J. Geophys. Res. Atmos. 118 (10), 4025–4048.
Wan, Z., Hook, S., Hulley, G., 2015. MYD11C3 MODIS/Aqua Land Surface Temperature/Emissivity Monthly L3 Global 0.05 Deg CMG V006. NASA EOSDIS Land Processes Distributed Active Archive Center.
Wigneron, J.P., et al., 2020. Tropical forests did not recover from the strong 2015–2016 El Niño event. Sci. Adv. 6 (6), eaay4603.
Xiao, X., et al., 2005. Satellite-based modeling of gross primary production in a seasonally moist tropical evergreen forest. Remote Sens. Environ. 94 (1), 105–122.
Xie, X., et al., 2022. Revisiting dry season vegetation dynamics in the Amazon rainforest using different satellite vegetation datasets. Agric. For. Meteorol. 312, 108704.
Xu, L., et al., 2011. Widespread decline in greenness of Amazonian vegetation due to the 2010 drought. Geophys. Res. Lett. 38 (7).
Yan, H., Wang, S.Q., Huete, A., Shugart, H.H., 2019. Effects of light component and water stress on photosynthesis of amazon rainforests during the 2015/2016 El Niño drought. J. Geophys. Res. Biogeosciences 124 (6), 1574–1590.
Yang, J., et al., 2018a. Amazon drought and forest response: largely reduced forest photosynthesis but slightly increased canopy greenness during the extreme drought of 2015/2016. Glob. Change Biol. 24 (5), 1919–1934.
Yang, Y., et al., 2018b. Post-drought decline of the Amazon carbon sink. Nat. Commun. 9 (1), 3172.
Yoshida, Y., et al., 2015. The 2010 Russian drought impact on satellite measurements of solar-induced chlorophyll fluorescence: insights from modeling and comparisons with parameters derived from satellite reflectances. Remote Sens. Environ. 166, 163–177.
Zhang, Y., Joiner, J., Alemohammad, S.H., Zhou, S., Gentine, P., 2018. A global spatially contiguous solar-induced fluorescence (CSIF) dataset using neural networks. Biogeosciences 15 (19), 5779–5800.
Zeng, N., et al., 2008. Causes and impacts of the 2005 Amazon drought. Environ. Res. Lett. 3 (1), 014002.
Zhang, Y., et al., 2013. Monitoring and estimating drought-induced impacts on forest structure, growth, function, and ecosystem services using remote-sensing data: recent progress and future challenges. Environ. Rev. 21 (2), 103–115.
Zhou, L., et al., 2014. Widespread decline of Congo rainforest greenness in the past decade. Nature 509 (7498), 86–90.
Zhou, S., Zhang, Y., Williams, A.P., Gentine, P., 2019. Projected increases in intensity, frequency, and terrestrial carbon costs of compound drought and aridity events. Sci. Adv. 5 (1), eaau5740.
Zhu, Z., et al., 2016. Greening of the Earth and its drivers. Nat. Clim. Change 6 (8), 791–795.